27th EPS Conference on Contr. Fusion and Plasma Phys. Budapest, 12-16 June 2000 ECA Vol. **24B** *(2000) 956 -959*

Density Dependence of Thermal Energy Confinement Properties of ELMy H-mode in JT-60U

H. Urano, Y. Kamada[1], H. Shirai[1], T. Takizuka[1], S. Ide[1], T. Fujita[1] and T. Fukuda[1]

Graduate School of Engineering, Hokkaido University, Sapporo 060-8628, JAPAN
[1]Naka Fusion Research Establishment, Japan Atomic Energy Research Institute
Naka-machi, Ibaraki 311-0193, JAPAN

1. Introduction

In tokamak reactor, high density operation with improved energy confinement of core plasma is required to achieve sufficiently high fusion gain. ITER is designed to operate ELMy H-mode discharges at a high density close to the Greenwald density limit n^{GW}. However, energy confinement (the *H*-factor) in ELMy H-mode has been observed to decrease with increasing density in many experiments [1-4]. Therefore, the clarification of the dominant causes of this degradation is the urgent issue in recent tokamak research. ELMs are considered to affect the energy confinement mainly by two basic mechanisms. One is the direct energy loss from the region near the plasma boundary. The other is an influence of the edge pedestal structure imposed by ELMs on the thermal energy confinement of the core plasmas. The stiff temperature profiles in ELMy H-mode plasmas, which are the evidence for an edge-core relationship, have been found on several devices [2,4-7].

2. Density dependence of the core and pedestal confinement

ELMy H-mode experiments were performed in JT-60U at I_p = 1.8 MA, where n^{GW} corresponds to $(8.1\text{-}8.7)\times10^{19}$ m^{-3}. The toroidal magnetic field B_t = 3.0 T and q_{95} = 2.9-3.1. Neutral beam injection (NBI) power P_{NBI} was scanned in steps from 4 to 13 MW. With deuterium gas puffing, the line-averaged electron density $\bar{n}_e$ was varied on a shot by shot from 2.4×10^{19} to 4.5×10^{19} m^{-3}. The maximum $\bar{n}_e$ reached was $(0.50\text{-}0.53)\times n^{GW}$. Elongation κ of 1.48 to 1.55 and triangularity δ of 0.16 to 0.19 were fixed. The plasma volume V_p is in the range of 60-63 m^3. The plasma major radius R_p and the minor radius a_p were in the ranges of 3.24-3.25 m and of 0.81-0.85 m, respectively. Figure 1 shows the *H*-factors of ELMy H-mode plasmas with P_{NBI} = 8-13 MW as a function of $\bar{n}_e / n^{GW}$. The *H*-factor of thermal plasma, $H_{th}^{L(JT\text{-}60)}$ [8], decreases continuously from 1.6 to 1.0 with an increase in $\bar{n}_e / n^{GW}$ from 0.30 to 0.53. In low density plasmas, high βp H-mode is observed in some cases where an internal transport barrier (ITB) is clearly formed. Figure 2(a) and (b) plot the electron density at the shoulder of the H-mode pedestal, n_e^{ped}, and at the center, $n_e(0)$, as a function of $\bar{n}_e$. In type-I ELMy phase, n_e^{ped} and $n_e(0)$ increase in proportion to $\bar{n}_e$. The electron and ion temperatures at the shoulder, or T_e^{ped} and T_i^{ped}, decrease from 1.6 to 0.8 keV and from 2.8 to 1.0 keV, respectively (see figure 2(c)). The central temperature of ions, $T_i(0)$, gradually goes down to the central temperature of electrons, $T_e(0)$, with an increase in $\bar{n}_e$ as shown in figure 2(d).

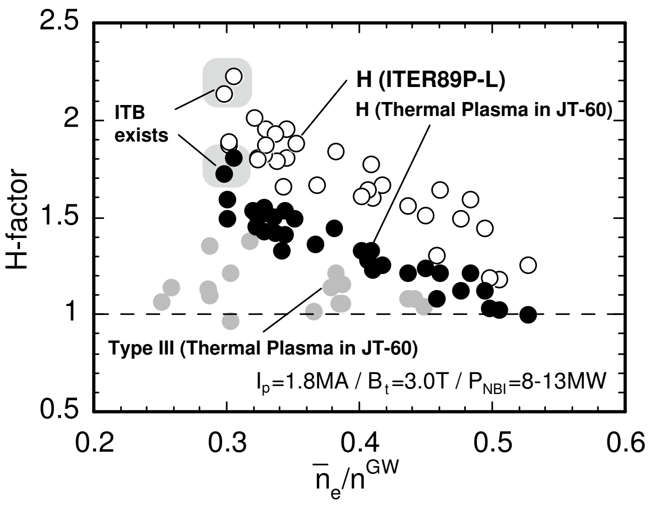

Fig.1 *H-factors for ELMy H-mode discharges in JT-60U as a function of* $\bar{n}_e / n^{GW}$

By evaluating the energy stored in the pedestal component, W_{th}^{ped}, and in the core component, W_{th}^{core}, their density dependences are shown in figure 3(a). Here, W_{th}^{ped} and W_{th}^{core} are given as:

$$W_{\rm th}^{\rm ped} = \frac{3}{2} k_{\rm B} V_{\rm p} \sum_j n_j^{\rm ped} T_j^{\rm ped} \qquad (1)$$

$$W_{\rm th}^{\rm core} = W_{\rm th} - W_{\rm th}^{\rm ped} \qquad (2)$$

With an increase in $\bar{n}_{\rm e}$ from 2.9×10^{19} to 4.5×10^{19} m^{-3} at $P_{\rm NBI}$ = 13.0 MW, $W_{\rm th}^{\rm ped}$ and $W_{\rm th}^{\rm core}$ are almost constant in the range of 0.8-0.9 MJ and of 1.2-1.5 MJ, respectively. However, it should be noted that $W_{\rm th}^{\rm core}$ increases in the low density region only with beam fueling: $\bar{n}_{\rm e} = (2.7\text{-}2.9)\times10^{19}$ m^{-3}. Figure 3(b) shows the enhancement factors of the core and edge pedestal confinement ($H_{\rm ONL}^{\rm core}$ and $H_{\rm ONL}^{\rm ped}$) based on the offset nonlinear scaling [9]. It is observed that $H_{\rm ONL}^{\rm ped}$ gradually decreases from 0.7 to 0.5 with an increase in $\bar{n}_{\rm e} / n^{\rm GW}$, while $H_{\rm ONL}^{\rm core}$ remarkably decreases from 1.3 to 0.8. Here, $H_{\rm ONL}^{\rm ped}$ is considerably small in these discharges. This result is observed at a low triangularity δ, in which the edge pressure gradient becomes small. Besides, it may be worth pointing out, in passing, that ITER H-mode confinement database predicts $H_{\rm ONL}^{\rm ped} \approx 0.75$ for JT-60U ELMy H-mode plasmas, where the pedestal component is statistically determined as the offset part of $W_{\rm th}$, independent of the heating power $P_{\rm abs}$ [9].

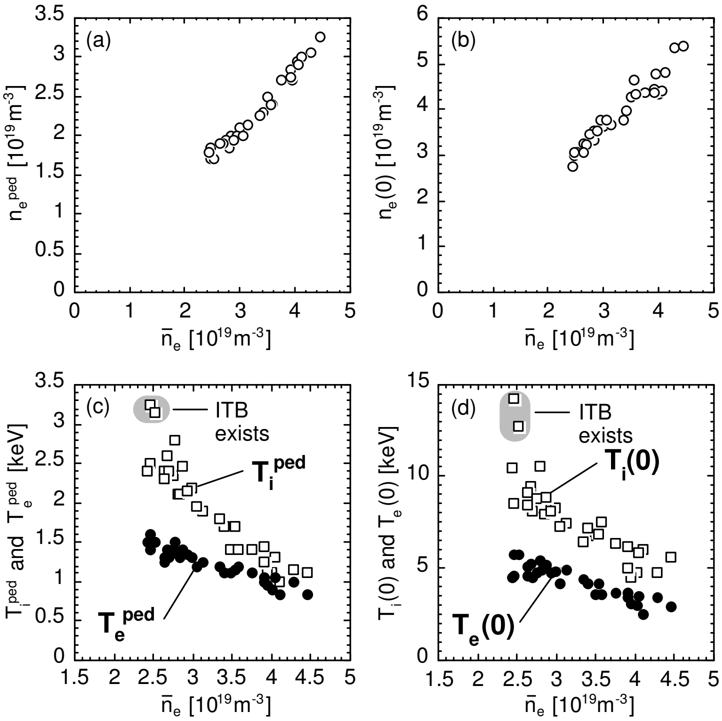

Fig.2 Density dependences of (a) $n_{\rm e}^{\rm ped}$, (b) $n_e(0)$, (c) $T_{\rm e}^{\rm ped}$ (closed circles), $T_{\rm i}^{\rm ped}$ (open squares) (d) $T_e(0)$ (closed circles) and $T_i(0)$ (open squares) in type-I ELMy phase.

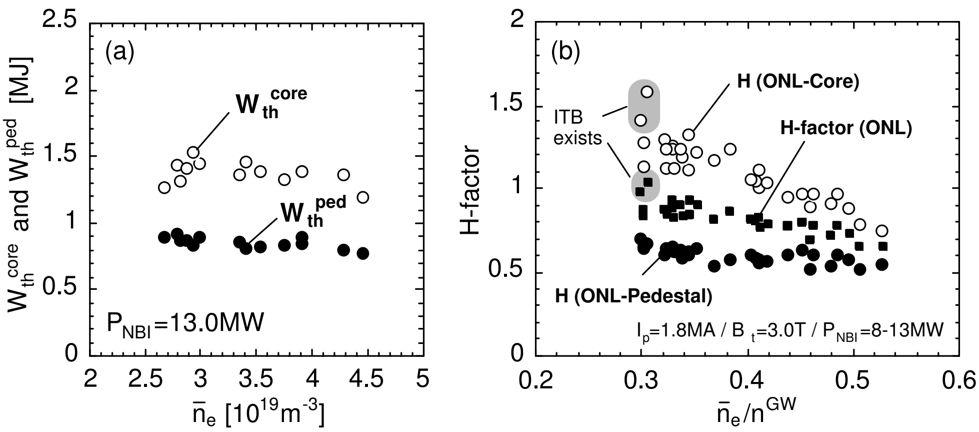

Fig.3 *(a) Density dependences of $W_{\rm th}^{\rm core}$ and $W_{\rm th}^{\rm ped}$ with P_{NBI} = 13.0MW. (b) H-factor in type-I ELMy phase based on the offset nonlinear scaling.*

3. Energy loss during type-I ELMs

The second point that requires clarification is a quantitative estimation of the direct energy loss due to ELM bursts. Figure 4 indicates the density dependences of the energy loss $\Delta W_{\rm ELM}$ during type-I ELMs, the energy stored outside the pedestal shoulder, $\Delta W_{\rm ped}$, and the ELM frequency $f_{\rm ELM}$. A gradual increase in $f_{\rm ELM}$ and a slight decrease or constancy in $\Delta W_{\rm ELM}$ were observed with increasing plasma density. If the magnetic structure is destroyed outside the shoulder of the H-mode pedestal and the energy stored in the edge plasma is expelled from the pedestal layer when an ELM burst occurs, then $\Delta W_{\rm ELM}$ and $\Delta W_{\rm ped}$ would have similar tendencies of the density dependence with each other. It should be noted that the time resolution of a diamagnetic measurement is not quite enough to analyze the ELM activity and the values of $\Delta W_{\rm ELM}$ may be underestimated by factor 2-3. Since it is reported that the reduction in the edge temperature due to the H-L back transition brought about the reduction in the core temperature in time scale much shorter than the energy confinement time $\tau_{\rm E}$ [10], ELMs are considered to be the phenomena not merely located at the edge plasma but there is a large transport structure connected with the core plasma.

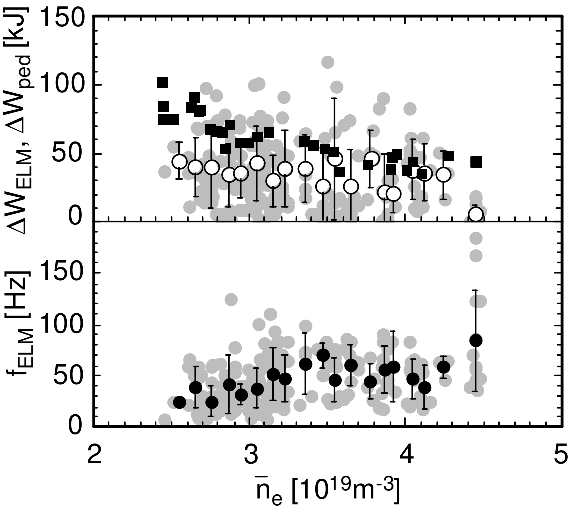

Fig.4 *Density dependences of $\Delta W_{\rm ELM}$ (open circles), $\Delta W_{\rm ped}$ (closed squares) and $f_{\rm ELM}$ (closed circles) during type-I ELMy phase.*

4. Correlation between the core and edge pedestal confinement

The classification of ELM behavior in ($n_{\rm e}^{\rm ped}$, $T_{\rm e}^{\rm ped}$) space is shown in figure 5. The arrow (i) indicates a relatively high density discharge. Both $n_{\rm e}^{\rm ped}$ and $T_{\rm e}^{\rm ped}$ increase through type-III ELM region with the heating power after the L-H transition, and type-I ELMs appear when $T_{\rm e}^{\rm ped}$ increases further with high power heating. In type-I ELMy phase, the increase in $n_{\rm e}^{\rm ped}$ accompanies the decrease in $T_{\rm e}^{\rm ped}$ so that the energy stored in the pedestal can be kept constant. The arrow (ii) indicates a relatively low density (no type-III phase) discharge. Since the L-H transition occurred at quite a low density, ELM-free phase has been sustained until type-I ELMs appeared. The confinement degradation can be linked to the relatively low pedestal temperatures because $n_{\rm e}^{\rm ped}$ and $T_{\rm e}^{\rm ped}$ correspond with each other in type-I ELMy phase. Figure 6(a) indicates the variations in $H_{\rm ONL}^{\rm core}$ and $H_{\rm ONL}^{\rm ped}$ in type-I ELMy phase as a function of $T_{\rm i}^{\rm ped}$. A coutinuous increase of $H_{\rm ONL}^{\rm core}$ is observed with an increase in $T_{\rm i}^{\rm ped}$ although the variation of $H_{\rm ONL}^{\rm ped}$ is small. However, $H_{\rm ONL}^{\rm core}$ is saturated with a further increase in $T_{\rm i}^{\rm ped}$. Here, it should be noted that the saturated region of *H*-factor corresponds to the low density region without deutrium gas puffing, in which $W_{\rm th}^{\rm core}$ can increase with the density as shown in figure 3(a).

The influence of the pedestal structure on thermal energy transport of the core plasma is evaluated by using the effective thermal conductivity of core component $\chi_{\rm eff}^{\rm core}$;

$$\chi_{\rm eff}^{\rm core} = -\frac{Q_{\rm core}}{\sum_j n_j \nabla T_j} \qquad (3)$$

where $Q_{\rm core}$ is a heat flux across the torus surface at $r_{\rm ped}$ and the temperature gradient ∇T was derived from $\Delta T(0)$ ($\equiv T(0) - T^{\rm ped}$) as a characteristic value which can determine the energy transport of the core plasma:

$$Q_{\rm core} = \frac{P_{\rm abs} - {\rm d}W/{\rm d}t}{4\pi^2 R_{\rm p} r_{\rm ped}} \qquad (4)$$

$$\sum_j n_j \nabla T_j \approx \sum_j n_j \frac{\Delta T_j(0)}{r_{\rm ped}} \qquad (5)$$

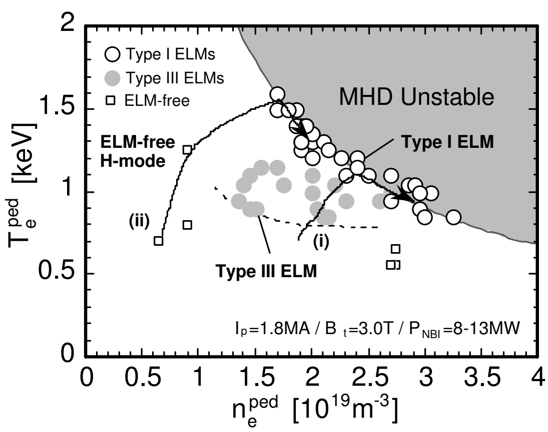

Fig.5 *Diagram of $n_{\rm e}^{\rm ped} - T_{\rm e}^{\rm ped}$ for classifying ELM behavior in JT-60U.*

In the low pedestal temperature region, $\chi_{\rm eff}^{\rm core}$ gradually decreases with an increase in $T_{\rm i}^{\rm ped}$ (see figure 6(b)). A slight increase or constancy of $\chi_{\rm eff}^{\rm core}$ is observed for $T_{\rm i}^{\rm ped} \geq 2.2$ keV as expected in figure 6(a). The reduction in $T^{\rm ped}$ caused by an increase in $n^{\rm ped}$ due to gas puffing seems to bring about the deterioration of the core energy confinement. In the low density region, however, it is observed that reduction in $T_{\rm i}^{\rm ped}$ does not necessarily cause the core confinement degradation. Conseqently, the pedestal temperature and density may play a significant role as the boundary condition in determining the thermal energy confinement of the core plasma. As a matter of fact, the energy confinement during H-mode depends in many cases strongly upon the temperature at the shoulder of the H-mode pedestal [2,4-7]. It follows from these observations that $T^{\rm ped}$ is expected to be the higher even at a high density if the higher sustainable $W_{\rm th}^{\rm ped}$ is produced. The large pedestal width and large $W_{\rm th}^{\rm ped}$ are obtained in ELMy H-mode plasmas with high triangularity. These discharges have achieved higher thermal energy confinement [11].

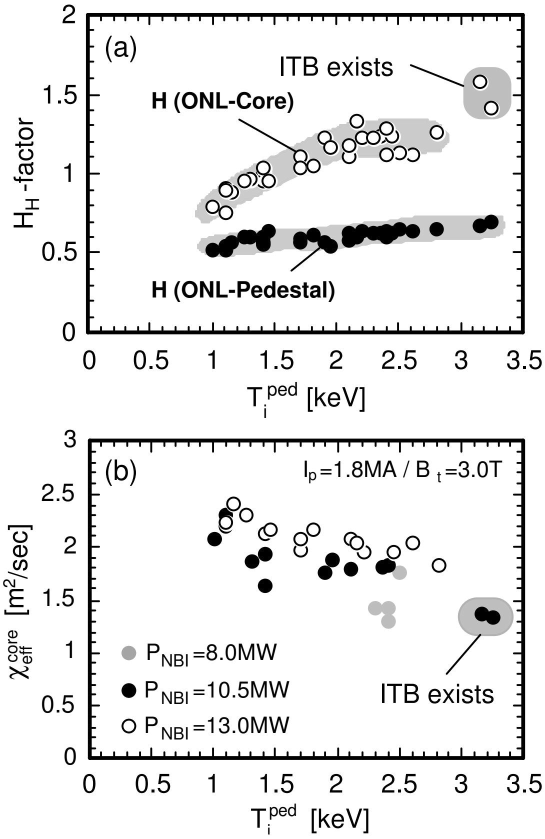

Fig.6 Dependences of (a) H (ONL-Core), H (ONL-Pedestal) and (b) $\chi_{\rm eff}^{\rm core}$ on $T_{\rm i}^{\rm ped}$ in type-I ELMy H-mode plasmas.

5. Conclusions

The dominant causes of the degradation of thermal energy confinement with increasing plasma density were analyzed in ELMy H-mode plasmas. Thermal energy stored in the pedestal, $W_{\rm th}^{\rm ped}$, is kept constant as the density is raised because of the action of type-I ELMs. The core component $W_{\rm th}^{\rm core}$ also tends to remain constant although the offset non-linear scaling predicts that $W_{\rm th}^{\rm core}$ should increase with density. Consequently, the enhancement factor of the core confinement remarkably decreases with $\bar{n}_{\rm e}$. When the density is increased by gas puffing, the saturation of $W_{\rm th}^{\rm ped}$ during type-I ELMs forces a reduction in $T^{\rm ped}$, which in turn leads to an increase in $\chi_{\rm eff}^{\rm core}$. An increase in the energy stored in the pedestal plasma due to high triangularity can produce thermally improved energy confinement even at a high density.

References

[1] JET Team: Nucl. Fusion **39** (1999) 1687.
[2] W. Suttrop, et al.: Proc. 17th Int. Conf. on Fusion Energy 1998, Yokohama (Vienna: IAEA) vol **2** (1999) 777.
[3] N. Asakura, et al.: Plasma Phys. Control. Fusion **39** (1997) 1295.
[4] H. Urano, et al.: submitted to Plasma Phys. Control. Fusion (2000).
[5] M. Greenwald, et al.: Nucl. Fusion **37** (1997) 793.
[6] W. Suttrop, et al.: Plasma Phys. Control. Fusion **39** (1997) 2051.
[7] G. Janeshitz, et al.: Proc. 26th EPS Conf. on Control. Fusion and Plasma Phys., Maastricht (Geneva: EPS) vol **23J** (1999) 1445.
[8] H. Shirai, et al. J. Phys. Soc. Japan **64** (1995) 4209.
[9] T. Takizuka: Plasma Phys. Control. Fusion **40** (1998) 851.
[10] S. V. Neudatchin: Jpn. J. Appl. Phys. **35** (1996) 3595.
[11] Y. Kamada, et al.: Proc. 16th Int. Conf. on Fusion Energy 1996, Montreal (Vienna: IAEA) vol **1** (1997) 247.